

Capacitance of a quantum dot from the channel-anisotropic two-channel Kondo model

Karyn Le Hur* and Georg Seelig†

Département de Physique Théorique, Université de Genève, CH-1211 Genève 4, Switzerland

(Received 25 November 2001; revised manuscript received 8 February 2002; published 15 April 2002)

We investigate the charge fluctuations of a large quantum dot coupled to a two-dimensional electron gas via a quantum point contact following the work of Matveev [K. A. Matveev, Phys. Rev. B **51**, 1743 (1995); Z. Éksp. Teor. Fiz. **98**, 1598 (1990) [Sov. Phys. JETP **72**, 892 (1991)]]. We limit our discussion to the case where exactly *two* channels enter the dot and we discuss the role of an anisotropy between the transmission coefficients (for these two channels) at the constriction. Experimentally, a channel anisotropy can be introduced by applying a relatively weak in-plane magnetic field to the system when only one “orbital” channel is open. The magnetic field leads to different transmission amplitudes for spin-up and spin-down electrons. In a strong magnetic field the anisotropic two-channel limit corresponds to two (spin polarized) orbital channels entering the dot. The physics of the charge fluctuations can be captured using a mapping on the channel-anisotropic two-channel Kondo model. For the case of weak reflection at the point contact this has already been briefly stressed by one of us [K. Le Hur, Phys. Rev. B **64**, 161302(R) (2001)]. This mapping is also appropriate to discuss the conductance behavior of a two-contact setup in strong magnetic field. Here, we elaborate on this approach and also discuss an alternative solution using a mapping on a channel-isotropic Kondo model. In addition we consider the limit of weak transmission. We show that the Coulomb-staircase behavior of the charge in the dot as a function of the gate voltage, is already smeared out by a small channel anisotropy both in the weak- and strong-transmission limits.

DOI: 10.1103/PhysRevB.65.165338

PACS number(s): 73.23.Hk, 72.15.Qm, 73.40.Gk, 72.10.Fk

I. INTRODUCTION

In the past few years a great amount of work has been devoted to studying the Kondo effect in mesoscopic systems.¹ A motivation for these efforts was the recent experimental observation of the Kondo effect in tunneling through a small quantum dot.^{2,3} In these experiments the effective (or excess) electronic spin of the dot acts as a magnetic impurity.

A different set of problems relating the Kondo effect to the physics of quantum dots is encountered when studying fluctuations of the charge of a large Coulomb-blockaded quantum dot. The setup we have in mind consists of a large quantum dot coupled to a reservoir via a quantum point contact (QPC) and capacitively coupled (with a capacitance C_{gd}) to a back gate (see Fig. 1). The amount of charge on the dot can be changed through the gate voltage V_G . The term “large” implies that the spacing Δ of the energy levels on the dot (almost) vanishes and is much smaller than the dot’s charging energy $E_C = e^2/(2C_{gd})$. We assume that the capacitance between the two-dimensional electron gas (2DEG) and the dot can be neglected.

There are two limits in which a mapping to a Kondo Hamiltonian can be used to calculate the charge on the quantum dot. These two limits roughly correspond to the cases of very strong and very weak reflection at the QPC. Before elaborating on this point we will give here the standard multichannel Kondo Hamiltonian,

$$H_K = H_{Kin} + \sum_{\alpha} \{ J_{\alpha,z} s_{\alpha,z}(0) S_z^i + J_{\alpha,\perp} [s_{\alpha,x}(0) S_x^i + s_{\alpha,y}(0) S_y^i] \} \quad (1)$$

in a very general form to be used as a point of reference for later discussions.⁴ Here \vec{S} is an impurity spin and $\vec{s}_{\alpha}(0)$ is the spin of conduction electrons with flavor α at the place of the impurity. We will consider only the two-channel case $\alpha = 1, 2$. In the discussion of the Coulomb-blockade problem we will encounter Kondo Hamiltonians that are both spin ($J_{\alpha,z} \neq J_{\alpha,\perp}$) and channel anisotropic ($J_{1,\perp} \neq J_{2,\perp}$).

We now want to return to the original problem and first want to discuss the limit of weak tunneling between the dot and the reservoir (strong reflection at the QPC). For low enough temperatures ($T \ll E_C$) the charge on the dot is quantized. When the gate voltage V_G is increased the charge on the dot changes in a steplike manner. This behavior is referred to as a Coulomb staircase. Charge fluctuations are important only for those values of the gate voltage at which two neighboring charge states (e.g., with n and $n+1$ electrons on the dot) are energy degenerate. Matveev demonstrated the equivalence of the effective Hamiltonian describing the charge dynamics close to such a degeneracy point to

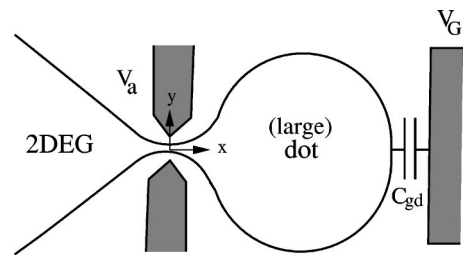


FIG. 1. A large quantum dot is coupled to a 2DEG via a quantum point contact. The number of electrons in the dot can be controlled through the gate voltage V_G . The auxiliary voltage V_a can be used to open or close the point contact and thus to adjust the reflection amplitudes for the transport channels in the QPC.

a spin-anisotropic Kondo Hamiltonian.⁵ If the dot and the reservoir are connected by m transport channels with the same transmission probability the problem can be mapped on a channel-isotropic m -channel Kondo model⁶ with $J_{\alpha,z}=0$ and $J_{\alpha,\perp}\ll 1$.⁵ The similarity of the charge dynamics on the dot to the spin dynamics in a Kondo model was already observed by Glazman and Matveev in their discussion on the conductance of a metallic grain (a quantum dot) tunnel coupled to two reservoirs.⁷

The limit of a point contact with one (electrons without spin) or two (electrons with spin) transport channels close to perfect transmission has also been treated. An effectively one-dimensional model for the dot-QPC system, which makes it possible to calculate the total charge on the dot using bosonization, was developed by Flensberg⁸ and by Matveev.⁹ Matveev⁹ also calculated the dot's capacitance as a function of the gate voltage and the reflection amplitude at the point contact. In his calculation he demonstrated that the Hamiltonian of the original problem can be mapped onto a Kondo Hamiltonian in the generalized Toulouse limit ($J_{1,z}=J_{2,z}=2\pi v_F$). In this limit the two-channel Kondo model is exactly solvable as was shown by Emery and Kivelson.¹⁰ It was one of the main results of Ref. 9 that Coulomb-blockade oscillations (accompanied by a logarithmic singularity in the expressions for the charge or the capacitance close to "half-integer" values of the number of electrons in the dot) persist also in the limit of weak reflection, as recently checked experimentally by Berman *et al.*¹¹ They are completely smeared out only if at least one transport channel is at perfect transmission, the charge in the dot then increases linearly with the gate voltage.^{8,9,12} A review of these results and more generally of interaction effects in quantum dots can be found in Ref. 13.

Extending our previous work¹⁴ we here want to discuss the effect of a *channel anisotropy* on the results for the capacitance in the two limits of almost perfect transmission and almost total reflection discussed above. We will show that the Coulomb-staircase behavior is smeared out by a small channel anisotropy both in the weak and strong reflection limit. We will concentrate on the case of two transport channels. Channel anisotropy then means that the reflection (or transmission) amplitudes for the two channels are different. Such a situation can be realized by applying a magnetic field to the sample. A weak in-plane magnetic field leads to different reflection amplitudes for spin-up and spin-down electrons. In a strong magnetic field electrons are spin polarized and the number of open channels in the QPC and their respective reflection amplitudes depend on the opening of the QPC. The confinement potential at the QPC and thus its opening can be tuned by changing the auxiliary gate voltage V_a (see Fig. 1). In the limit of small reflection an intuitive physical picture for the transition from the channel symmetric case⁹ to the case of a weak asymmetry between the two channels can be obtained¹⁴ from the use of the *channel-anisotropic* two-channel Kondo model at the Emery-Kivelson line.¹⁵ This model has also been investigated in Ref. 16. The two coupling constants of the asymmetric Kondo model are directly related to the reflection amplitudes of the two transport channels in the QPC. In this paper we

will elaborate on this mapping and discuss its limitations. Although the physical picture associated with the *channel-anisotropic* two-channel Kondo model is very appealing, the Coulomb-blockade problem in the high transparency limit with two transport channels with different reflection coefficients can also be solved through a mapping on the *channel-isotropic* two-channel Kondo model as we will show. Such a procedure was applied by Furusaki and Matveev¹⁷ when they calculated the inelastic cotunneling through a quantum dot strongly coupled to two quantum point contacts with one transport channel each (electrons in a strong magnetic field). We will see furthermore that in the case of tunnel coupling (small transmission) an asymmetry between transmission amplitudes of different channels will lead to a mapping of the Hamiltonian on a channel-anisotropic Kondo model with ($J_{1,z}=J_{2,z}=0$).

Our paper is structured as follows. In a first part we consider the weak coupling limit. We start by developing the model Hamiltonian in Sec. II. In Sec. III we discuss the mapping on the channel-anisotropic two-channel Kondo model and use it to calculate the capacitance of the quantum dot in a weak magnetic field. In Sec. IV we show that the same results can also be found from a mapping to a channel-isotropic Kondo model and in addition look at the case of a strong magnetic field applied to the QPC-dot system. In Sec. V a simple scaling argument is used to rederive the main (exact) results of Secs. III and IV. In Sec. VI, we will show that the channel-anisotropic two-channel Kondo model can also be used to discuss the conductance in a two-contact setup with a strong in-plane magnetic field. The limit of small transmission through the quantum dot will finally be considered in Sec. VII.

II. THE MODEL

We consider here a large quantum dot weakly coupled to a 2DEG via a point contact⁹ (see Fig. 1). The shape of the QPC is defined through metallic gates put on top of a 2DEG. The lateral confinement potential in the QPC can be controlled by changing the voltage applied to these gates. As a consequence of the lateral confinement the conductance of the QPC is quantized and electron motion in the vicinity of the QPC is essentially one dimensional. The one-dimensional wave-function Ψ_σ^n for motion along the x axis is characterized by the spin index $\sigma=\uparrow,\downarrow$ and the (orbital) channel quantum number n due to the lateral confinement.¹⁸ Note, that from here on we will use the word channel to mean electrons with a certain pair of indices σ,n . As a short notation we introduce the channel index $\alpha=\sigma,n$ and we denote the wave function of an electron in this channel by Ψ_α . In the further analysis we neglect transport channels that are totally reflected at the QPC, since electrons from these channels are confined to the reservoir and will not contribute to the charging of the dot. We will concentrate on the case where only two channels are open. This can be realized in two different ways. If a weak (or zero) in-plane magnetic field is applied (see Sec. III), the two channels correspond to the two spin polarizations of electrons in the lowest ($n=1$) energy eigenstate of the lateral Hamiltonian ($\Psi_1=\Psi_\uparrow^1, \Psi_2$

$=\Psi_{\downarrow}^1$). The role of the magnetic field is to introduce an asymmetry between the reflection coefficients for spin-up and spin-down electrons.¹⁴ In a strong magnetic field the electrons are spin-polarized and the two-channel case corresponds to two orbital channels entering the constriction (e.g., $\Psi_1 = \Psi_{\uparrow}^1, \Psi_2 = \Psi_{\uparrow}^2$); see Sec. IV.

Since we are interested in energies much smaller than the Fermi energy, we linearize the spectrum around the Fermi points. Furthermore, it is convenient to decompose the wave function into a right-going and a left-going contribution $\Psi_{\alpha} = \exp(ik_F x)\Psi_{\alpha,R}(x) + \exp(-ik_F x)\Psi_{\alpha,L}(x)$. For two open transport channels the Hamiltonian for the electrons in the point contact is

$$H_{Kin} = -iv_F \sum_{\alpha=1,2} \int_{-\infty}^{\infty} dx [\Psi_{\alpha,R}^{\dagger}(x) \partial_x \Psi_{\alpha,R}(x) - \Psi_{\alpha,L}^{\dagger}(x) \partial_x \Psi_{\alpha,L}(x)], \quad (2)$$

where the sum is over (open) quantum channels. Electron interactions in the quantum dot are taken into account via the Coulomb Hamiltonian

$$H_C = E_C(Q - N)^2 - E_C N^2. \quad (3)$$

The parameter $eN = V_G C_{gd}$ is proportional to the gate voltage and $E_C = e^2/(2C_{gd})$ is the charging energy. In addition we allow for a weak backscattering²⁹ in the point contact:

$$H_{bs} = v_F \sum_{\alpha=1,2} |r_{\alpha}| [\Psi_{\alpha,R}^{\dagger}(0)\Psi_{\alpha,L}(0) + \text{H.c.}]. \quad (4)$$

The transmission is supposed to be globally adiabatic.¹⁹ The reflection amplitudes $|r_1|$ and $|r_2|$ can be tuned applying a voltage to the gates defining the QPC. The main goal in the following will be to calculate the shift in the ground-state energy $\delta\epsilon$ due to the backscattering in the point contact. From the correction $\delta\epsilon$ it is possible to obtain the average charge in the dot and the dot's capacitance via

$$\langle Q \rangle = C_{gd} V_G - \frac{\partial(\delta\epsilon)}{\partial V_G},$$

$$C = \frac{\partial\langle Q \rangle}{\partial V_G} = C_{gd} - \frac{\partial^2(\delta\epsilon)}{\partial V_G^2}. \quad (5)$$

To manipulate the Hamiltonian of the one-dimensional interacting system we have introduced above, it is convenient to use the bosonization technique. Bosonizing in the standard way we express the Fermi field operators through the bosonic fields $\phi_{\alpha}(x)$ and $\theta_{\alpha}(x)$ and write^{20,21}

$$\Psi_{\alpha,R/L}(x) = \frac{1}{\sqrt{2\pi a}} \exp\{i\sqrt{\pi}[-p\phi_{\alpha}(x) + \theta_{\alpha}(x)]\}. \quad (6)$$

Here $p=1$ for right movers (R) and $p=-1$ for left movers (L). The bosonic fields obey the commutation relations

$$[\phi_{\alpha}(x), \theta_{\beta}(y)] = \frac{i}{2} \text{sgn}(x-y) \delta_{\alpha,\beta},$$

$$[\phi_{\alpha}(x), \partial_y \theta_{\beta}(y)] = i \delta(x-y) \delta_{\alpha,\beta},$$

$$[\phi_{\alpha}(x), \phi_{\beta}(y)] = [\theta_{\alpha}(x), \theta_{\beta}(y)] = 0. \quad (7)$$

In the new variables the kinetic energy takes the form

$$H_{Kin} = v_F \sum_{\alpha=1,2} \int_{-\infty}^{\infty} dx [(\partial_x \phi_{\alpha})^2 + (\partial_x \theta_{\alpha})^2]. \quad (8)$$

To bosonize the Coulomb Hamiltonian we use the relation: $\Psi_{\alpha,L}^{\dagger}\Psi_{\alpha,L} + \Psi_{\alpha,R}^{\dagger}\Psi_{\alpha,R} := -\partial_x \phi_{\alpha}/\sqrt{\pi}$. The total charge in the dot then is

$$Q = \sum_{\alpha=1,2} \int_0^{\infty} dx (:\Psi_{\alpha,R}^{\dagger}\Psi_{\alpha,R} + \Psi_{\alpha,L}^{\dagger}\Psi_{\alpha,L}:). \quad (9)$$

The charge in the dot is now measured in units of e . We neglect both finite-size effects in the dot^{13,22} (supposed to be ideal with no dephasing process) and mesoscopic corrections to the capacitance C_{gd} .^{23,24} Expressing the charge in terms of the bosonic variables we obtain $Q = [\phi_1(0) + \phi_2(0)]/\sqrt{\pi}$. The term at spatial infinity is independent of the gate voltage. We choose $\phi_i(\infty) = 0$ in such a way that the total charge Q on the dot is zero when $N=0$. Consequently we get

$$H_C = \frac{E_C}{\pi} \left(\sum_{\alpha=1,2} \phi_{\alpha}(0) - \sqrt{\pi}N \right)^2 \quad (10)$$

for the Coulomb Hamiltonian. In writing Eq. (10) we have only considered the Q -dependent part of Eq. (3). Finally we also have to bosonize the backscattering Hamiltonian, which leads us to

$$H_{bs} = \frac{v_F}{\pi a} \sum_{\alpha=1,2} |r_{\alpha}| \cos[\sqrt{4\pi}\phi_{\alpha}(0)]. \quad (11)$$

Now we introduce the new standard variables $\phi_{c,s} = (1/\sqrt{2})[\phi_1(x) \pm \phi_2(x)]$ and $\theta_{c,s} = (1/\sqrt{2})[\theta_1(x) \pm \theta_2(x)]$ where the positive sign belongs to the label c (charge) and the negative sign belongs to s (spin). Note that in the case of a strong magnetic field electrons are spin polarized. The index s then labels a ‘‘pseudospin’’ and not physical spin states. The kinetic energy in the new variables has the standard form of Eq. (8). The Coulomb Hamiltonian

$$H_C = \frac{2E_C}{\pi} [\phi_c(0) - \sqrt{\pi/2}N]^2 \quad (12)$$

is a function of the charge field only which is the main motivation for the introduction of this new set of variables. Furthermore we get for the backscattering part

$$H_{bs} = \frac{v_F}{\pi a} (|r_1| + |r_2|) \cos[\sqrt{2\pi}\phi_c(0)] \cos[\sqrt{2\pi}\phi_s(0)] - \frac{v_F}{\pi a} (|r_1| - |r_2|) \sin[\sqrt{2\pi}\phi_c(0)] \sin[\sqrt{2\pi}\phi_s(0)]. \quad (13)$$

We now introduce the charge fluctuation field $\hat{\phi}_c(0) = \phi_c(0) - \sqrt{\pi/2}N$. The total charge in the dot is pinned at its classical value $Q_{cl} = \phi_c(0) = \sqrt{\pi/2}N$ to minimize the Coulomb energy. For weak backscattering $|r_1|, |r_2| \ll 1$ and for energies below the charging energy we can average over the charge fluctuations $\hat{\phi}_c(0)$. When averaging over the term $\cos[\sqrt{2\pi}\phi_c(0)] = \cos[\sqrt{2\pi}\hat{\phi}_c(0) + \pi N]$ in Eq. (13) we obtain the expression

$$e^{-\pi(\hat{\phi}_c(0)^2)} \cos(\pi N) = \sqrt{\frac{a\gamma E_C}{v_F}} \cos(\pi N). \quad (14)$$

Here the angular brackets mean averaging with regard to the ground state of the free Hamiltonian Eq. (8). An analogous expression can also be found for the term $\sin[\sqrt{2\pi}\phi_c(0)]$ in Eq. (13). When calculating the correlator

$$\langle \hat{\phi}_c(0)^2 \rangle = -\frac{1}{2\pi} \ln \frac{a\gamma E_C}{v_F} \quad (15)$$

we have taken into account that only fluctuation modes with energies larger than the charging energy E_C can enter into the dot. Here γ is defined through $\gamma = e^C$ where $C \approx 0.577$ is Euler's constant. After the averaging, the backscattering part of the Hamiltonian can thus be written as

$$H_{bs} = \frac{\sqrt{\gamma a E_C v_F}}{\pi a} (|r_1| + |r_2|) \cos(\pi N) \cos[\sqrt{2\pi}\phi_s(0)] - \frac{\sqrt{\gamma a E_C v_F}}{\pi a} (|r_1| - |r_2|) \sin(\pi N) \sin[\sqrt{2\pi}\phi_s(0)]. \quad (16)$$

Using simple trigonometric relations the Hamiltonian Eq. (16) can be rewritten in an alternative form¹⁷ as

$$H_{bs} = \frac{\sqrt{a\gamma E_C v_F}}{\pi a} (r e^{i\sqrt{2\pi}\phi_s(0)} + r^* e^{-i\sqrt{2\pi}\phi_s(0)}), \quad (17)$$

where r is the complex parameter $r = (|r_1| e^{i\pi N} + |r_2| e^{-i\pi N})/2$. The first form of the backscattering term Eq. (16) will be used in Sec. III when discussing the two-channel anisotropic version of the Kondo model, while Eq. (17) will be useful as a starting point for the mapping on the isotropic form of the two-channel Kondo model (see Sec. IV). The charge part of the kinetic energy can now be dropped since it is completely decoupled from the perturbation due to the backscattering.

III. CHANNEL-ANISOTROPIC TWO-CHANNEL KONDO MODEL

In this section we will concentrate exclusively on the case where the reflection amplitudes $|r_1|$ and $|r_2|$ are very close to each other. It is then convenient to introduce the parameters $|R| = |r_1| + |r_2|$ and $|\delta r| = |r_2| - |r_1|$ where $|\delta r| \ll |R| \ll 1$. For the sake of clarity we have split up this section into three subsections. In the first subsection we will discuss the relation between our problem and the channel-anisotropic (two-channel) Kondo model.¹⁴ In the second subsection we will derive an expression for the impurity correction to the ground-state energy while a physical realization of the case $|\delta r| \ll |R| \ll 1$ is discussed in the third subsection. There we will also explicitly calculate the charge in the dot and the dot's capacitance.

A. Equivalence to the Kondo model

We will now see that our theory for the Coulomb-blockade problem can be mapped on the anisotropic two-channel Kondo model at the Emery-Kivelson line, i.e., $J_{\sigma,z} = 2\pi v_F$ with $\sigma = 1, 2$. The solution of this model^{15,25} was given by Fabrizio, Gogolin, and Nozières.¹⁵

Introducing the auxiliary impurity-spin operators \hat{S}_x and \hat{S}_y we rewrite the backscattering term [Eq. (16)] as

$$H_{bs} = \frac{J_x}{\pi a} \cos[\sqrt{2\pi}\phi_s(0)] \hat{S}_x + \frac{J_y}{\pi a} \sin[\sqrt{2\pi}\phi_s(0)] \hat{S}_y, \quad (18)$$

where the Kondo coupling parameters are defined through

$$J_x = 2|R| \sqrt{a\gamma E_C v_F} \cos(\pi N), \quad J_y = 2|\delta r| \sqrt{a\gamma E_C v_F} \sin(\pi N). \quad (19)$$

Starting with a standard Kondo model, we rather get $J_x \propto (J_{1\perp} + J_{2\perp})$ and $J_y \propto (J_{1\perp} - J_{2\perp})$, where $J_{\sigma,\perp}$ denotes the transverse Kondo coupling of each conduction-band channel with the magnetic impurity. The total Hamiltonian, which we will denote H_{EK}^A , is given by $H_{EK}^A = H_{Kin}(\phi_s, \theta_s) + H_{bs}(\phi_s)$, where the kinetic term is of the form Eq. (8). Both \hat{S}_x and \hat{S}_y can be considered as good quantum numbers since their commutators with the Hamiltonian H_{EK}^A are small, close to perfect transmission through the quantum point contact:

$$[H_{EK}^A, \hat{S}_x] \propto -i|R|\hat{S}_z, \quad [H_{EK}^A, \hat{S}_y] \propto i|\delta r|\hat{S}_z. \quad (20)$$

The impurity spin in H_{EK}^A can oscillate between the two values $\hat{S}_x = 1/2$ and $\hat{S}_y = -1/2$. It is important to note that the backscattering part of the total Hamiltonian [Eq. (16)] and the coupling term of the two-channel anisotropic Kondo model [Eq. (18)] are exactly equivalent only in the channel symmetric case $|\delta r| = 0$, since \hat{S}_x and \hat{S}_y do not commute. However, we will see in the following section that the ap-

proximation made in writing Eq. (18) is good as long as $|\delta r| \ll |R|$ or $N \sim 0, \pm 1/2, \pm 1 \dots$

We now want to find the shift of the energy due to the backscattering or, in the language of the Kondo problem, the impurity correction to the ground-state energy. To make further progress it is useful to refermionize the Hamiltonian. The basic idea is to introduce a unique operator $\psi(x)$ such that $\cos[\sqrt{2\pi}\phi_s(0)] \propto \psi(0) + \psi^\dagger(0)$ and $\sin[\sqrt{2\pi}\phi_s(0)] \propto \psi(0) - \psi^\dagger(0)$. Furthermore, we use the Majorana representation

$$\begin{aligned}\sqrt{2}\hat{S}_x &= a = (d + d^\dagger)/\sqrt{2}, \\ \sqrt{2}\hat{S}_y &= -b = (d^\dagger - d)/(i\sqrt{2}),\end{aligned}\quad (21)$$

to express the spin operators through fermionic operators. The d operators ($d = a + ib$) obey $\{d^\dagger, d\} = 1$ and $\{d, \psi(x)\} = 0$. The (unusual) refermionization procedure will be extensively discussed in Appendix A. There we also give a precise definition of the new fermionic fields ψ . After refermionization the kinetic energy takes the standard form

$$H_{Kin} = -iv_F \int_{-\infty}^{\infty} dx \psi^\dagger(x) \partial_x \psi(x), \quad (22)$$

while the backscattering Hamiltonian is

$$H_{bs} = \frac{iJ_x}{\sqrt{4\pi a}} [\psi(0) + \psi^\dagger(0)]b + \frac{J_y}{\sqrt{4\pi a}} [\psi(0) - \psi^\dagger(0)]a. \quad (23)$$

So we finally arrive at a (standard) solvable resonant level type of model for the two Majorana fermions a and b .^{15,25}

B. Impurity corrections and scattering phase shifts

Our next step is to calculate the impurity corrections to the ground-state energy from the impurity Green's functions $G_a = -\langle T_\tau a(\tau)a(0) \rangle$ and $G_b = -\langle T_\tau b(\tau)b(0) \rangle$. The Fourier transforms of these Green's functions can be found in a convenient way from the equations of motion (cf. Appendix B). We get

$$G_k(\omega) = \frac{1}{\omega + i\Gamma_k \operatorname{sgn}(\omega)}, \quad (24)$$

where the label k is $k = a, b$. The width of the resonant $a(b)$ level $\Gamma_a(\Gamma_b)$ is related to the respective Kondo coupling constant $J_y(J_x)$ via

$$\begin{aligned}\Gamma_a &= \frac{J_y^2}{4\pi a v_F} = \frac{E_C \gamma}{\pi} |\delta r|^2 \sin^2(\pi N), \\ \Gamma_b &= \frac{J_x^2}{4\pi a v_F} = \frac{E_C \gamma}{\pi} |R|^2 \cos^2(\pi N).\end{aligned}\quad (25)$$

The impurity correction to the ground-state energy at zero temperature is

$$\delta\epsilon = - \int_{\omega_{min}}^{E_C} \frac{d\omega}{2\pi} \omega [n_a(\omega) + n_b(\omega)]. \quad (26)$$

The occurrence of a high-energy cutoff at E_C in Eq. (26) is an intrinsic property of the theory developed so far. The low-energy cutoff ω_{min} needs some additional explanation. We can distinguish two different situations. In the neighborhood of integer values of N the resonance width Γ_a is negligibly small. Already at temperatures of the order of Γ_b spin fluctuations will get pinned, since the coupling constant J_x goes to strong coupling (compare Sec. V).

Very close to half-integer values of N , however, we have $\Gamma_b \ll \Gamma_a$ even though $|\delta r| \ll |R|$. Thus the coupling J_y will go to strong coupling before J_x and spin fluctuations will be frozen at Γ_a . An expression for ω_{min} that correctly reproduces these two limits is $\omega_{min} = \max\{\Gamma_a, \Gamma_b\}$. The density of states $n_k(\omega)$ of impurity k in Eq. (26) is related to the corresponding impurity Green's function through

$$n_k(\omega) = -2 \operatorname{Im}\{G_k(\omega)\} = \frac{2\Gamma_k \operatorname{sgn}(\omega)}{\omega^2 + \Gamma_k^2}. \quad (27)$$

With this expression for $n_k(\omega)$ the integration in Eq. (26) can easily be performed and we get

$$\delta\epsilon = - \frac{1}{2\pi} \sum_{k=a,b} \left[\Gamma_k \ln \left(\frac{E_C^2 + \Gamma_k^2}{\max\{\Gamma_a, \Gamma_b\}^2 + \Gamma_k^2} \right) \right]. \quad (28)$$

For most purposes it is sufficient to approximate this expression by the more simple form²⁶

$$\delta\epsilon = - \frac{1}{\pi} (\Gamma_a + \Gamma_b) \ln \left(\frac{E_C}{\max\{\Gamma_a, \Gamma_b\}} \right). \quad (29)$$

We have used $\Gamma_k \ll E_C$ and have dropped an additive constant. A quantity that is interesting is the scattering phase shift (extracted from the Friedel sum rule)

$$\delta(\omega) = \frac{1}{2} \sum_{k=a,b} \arctan \left(\frac{\Gamma_k}{\omega} \right) \quad (30)$$

of the conduction electrons ψ due to the impurity scattering. In the channel symmetric case we have $\Gamma_a = 0$ and $\delta(\omega \ll \Gamma_b) = \pi/4$. The Friedel sum rule can also be rewritten $Z = 2\sum_l (2l+1) \delta/\pi$ where Z is the impurity charge screened by the electrons. For s -wave scattering ($l=0$) and $Z=1/2$ we recover $\delta = \pi/4$. The particular value of δ can thus be understood as a consequence of the fact that only ‘‘half’’ of the fermion d (the part a) is coupled to the conduction electrons. In general, if both Γ_a and Γ_b are finite we find $\delta = \pi/2$ in the limit $\omega \rightarrow 0$ and $Z=1$ since now a and b are screened. Here, (even) for a *finite* channel asymmetry, we still find $\delta = \pi/4$ at the fixed point because close to $N=1/2$ we have $\Gamma_b \rightarrow 0$ and close to $N=0, \pm 1$ we have $\Gamma_a \rightarrow 0$. This gives a physical justification on the validity of the mapping in Sec. IV. It is important to remember that the ‘‘spin fermions’’ ψ are not the real electrons but are related to the spin degrees of freedom of the original electronic wave functions. However, they play the part of the conduction electrons of the real Kondo

problem. In the case of spinless electrons (electrons in a strong magnetic field) and for a single transmitted channel $|r| \ll 1$ the scattering phase shift of the real electrons is related to the average charge on the dot via $\delta = \pi \langle Q \rangle$, again as a consequence of Friedel's rule. It was shown by Aleiner and Glazman²² that in the one-channel limit this relation can be used to calculate the impurity correction [see Eq. (35)] in an intuitive way. The physics resembles closely the one of the one-channel Kondo problem.²⁷

C. Applications

The case $|\delta r| \ll |R| \ll 1$ can be realized in our setup by applying a weak in-plane magnetic field. In a nonzero field the reflection amplitudes $|r_1|$ and $|r_2|$ for electrons with spin up and spin down are different due to the Zeeman effect. The channel index α here distinguishes between spin-up and spin-down electrons in the lowest orbital channel $n=1$. The (original) electronic wave functions for electrons in the two channels are $\Psi_{\alpha=1} = \Psi_{\uparrow}^{n=1}$ and $\Psi_{\alpha=2} = \Psi_{\downarrow}^{n=1}$. We first want to consider the special case of zero magnetic field, which was solved by Matveev in Ref. 9. The reflection amplitudes for the two channels, corresponding to spin-up and spin-down electrons are equal ($|r_1| = |r_2| = |R|/2$) and thus $|\delta r| = 0$. It follows from Eqs. (19) and (25) that $J_y = 0$ and $\Gamma_a = 0$. Furthermore, from Eq. (25) we know that $\Gamma_b = |R|^2 \gamma E_C \cos^2(\pi N) / \pi$. Calculating the energy with Eq. (29) we find⁹

$$\delta\epsilon = + \frac{\gamma E_C}{\pi^2} |R|^2 \cos^2(\pi N) \ln[\gamma / \pi |R|^2 \cos^2(\pi N)]. \quad (31)$$

The correction to the capacitance can then easily be calculated using Eq. (5) and is found to be

$$\delta C = -2 \gamma E_C |R|^2 \beta^2 \cos(2\pi N) \ln\left(\frac{1}{|R|^2 \cos^2(\pi N)}\right). \quad (32)$$

Here we have kept only the logarithmically divergent contribution that will dominate all other terms close to $N=1/2$. The parameter $\beta = e/(2E_C)$ is the ratio of the dimensionless parameter N and the gate voltage V_G , $\beta = N/V_G$. This seems to be in agreement with the recent capacitance experiment of Ref. 11.

As we can see from Eq. (18) in the channel-symmetric case only fermion b is coupled to the field ψ . If we allow for a weak magnetic field the reflection coefficients for spin-up and spin-down electrons are slightly different and $|\delta r| \neq 0$. As a consequence the Kondo coupling J_y does not vanish anymore and both Majorana fermions a and b are coupled to the bath. The total energy shift $\delta\epsilon$ from Eqs. (25) and (29) is found to be¹⁴

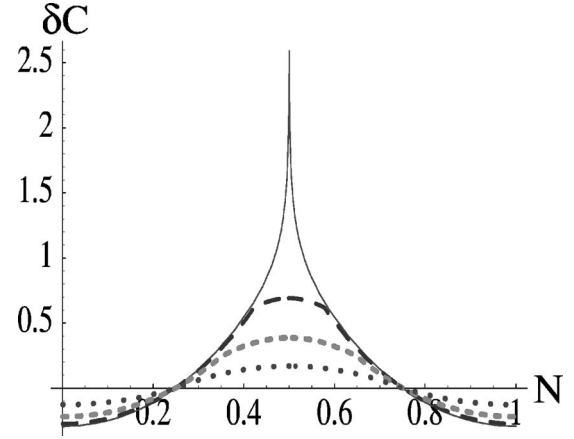


FIG. 2. The correction to the capacitance Eq. (34) is shown for different values of the anisotropy parameter $|\delta r| = |r_2| - |r_1|$. The parameter $|R| = |r_1| + |r_2|$ is set to $|R| = 0.4$. The solid line corresponds to the channel isotropic case $|\delta r| = 0$ where the capacitance is logarithmically divergent. In order of decreasing peak height the remaining three curves correspond to $|\delta r| = 0.1$, $|\delta r| = 0.2$, and $|\delta r| = 0.3$. The units of the capacitance are arbitrary.

$$\begin{aligned} \delta\epsilon = & + \frac{\gamma E_C}{\pi^2} [|R|^2 \cos^2(\pi N) + |\delta r|^2 \sin^2(\pi N)] \\ & \times \ln[\gamma / \pi \max\{|\delta r|^2 \sin^2(\pi N), |R|^2 \cos^2(\pi N)\}]. \end{aligned} \quad (33)$$

Due to the appearance of the max the logarithm does not diverge anymore. Still it can be very large due to the smallness of $|\delta r|$ and the logarithmic term will dominate in the capacitance (See Fig. 2):

$$\begin{aligned} \delta C = & -2 \gamma E_C \beta^2 (|R|^2 - |\delta r|^2) \cos(2\pi N) \\ & \times \ln\left(\frac{1}{\max\{|\delta r|^2 \sin^2(\pi N), |R|^2 \cos^2(\pi N)\}}\right). \end{aligned} \quad (34)$$

We see from Eqs. (33) and (34) that an arbitrary weak anisotropy between the two reflection coefficients is sufficient to cut off the logarithmic divergence. At the degeneracy point $N=1/2$, we find $\delta C \propto \ln|\delta r|$. There is some analogy⁹ with the behavior of the magnetic susceptibility of the impurity $\chi = \partial^2(\delta\epsilon)/\partial h^2$ away from the Emery-Kivelson line¹⁵ and with that of the local magnetic susceptibility $\chi_l = \partial\langle \hat{S}_z \rangle / \partial h$ at the Emery-Kivelson line (the magnetic field h would only act on the impurity),²⁵ even though for weak backscattering at the QPC there is no real correspondence between the charge in the dot Q and \hat{S}_z . From the two-channel anisotropic Kondo model we see that the appearance of the second energy scale that leads to the suppression of the divergence follows in a natural manner from the coupling of the second Majorana fermion to the conduction electrons.

At this point it is also interesting to compare these results to the result obtained in the case of a single transmitted channel (reflection amplitude $|r_1| \ll 1$ and $|r_2| \rightarrow 1$). Such a situ-

ation can be realized in a strong magnetic field¹⁴ (spinless electrons) and was also treated in Ref. 9. The energy shift for this case is

$$\delta\epsilon \propto |r_1| E_C \cos(2\pi N) \quad (35)$$

and therefore no logarithmic contribution occurs anymore in the expressions for the charge and the capacitance. We only get a periodic oscillation as a function of the gate voltage.

In the following section we want to demonstrate that the approximation made in writing Eq. (18) is justified. Furthermore, we will address the case of strong asymmetry between the conduction channels.

IV. MAPPING TO A CHANNEL-ISOTROPIC KONDO MODEL

We have seen in the preceding section that the backscattering term Eq. (18) is not exactly equivalent to the original Hamiltonian Eq. (16). We will now justify the approximation made and will rederive the results we have found from the two-channel anisotropic Kondo model in an exact way, following in our derivation Furusaki and Matveev.¹⁷ This section is structured in a similar way as Sec. III. The mathematical mapping will be discussed in a first subsection while a second short subsection will be devoted to the discussion of an application.

A. Mapping

As a starting point we use the form Eq. (17) of the original backscattering Hamiltonian, which we rewrite as

$$H_{bs} = \frac{J_0}{2\pi a} (r e^{i\sqrt{2}\pi\phi_s(0)} + r^* e^{-i\sqrt{2}\pi\phi_s(0)}) \hat{S}_x. \quad (36)$$

Here r is the complex parameter $r = (|r_1| e^{i\pi N} + |r_2| e^{-i\pi N})/2$ and $J_0 = 4\sqrt{a\gamma E_C v_F}$. Exactly as in the preceding section we have introduced an auxiliary impurity spin \hat{S}_x . The spin \hat{S}_x is a good quantum number since it commutes with the total Hamiltonian (here $\hat{S}_x = 1/2$). It is important to note that therefore Eq. (36) is exactly equivalent to the original expression Eq. (17). Reformionizing as described in Appendix A gives

$$H_{bs} = \frac{iJ_0}{\sqrt{4\pi a}} [r\psi(0) + r^*\psi^\dagger(0)]b, \quad (37)$$

where we again use the Majorana representation for the impurity spin. The Hamiltonian Eq. (37) is very similar to the resonant level model that occurs in the solution of the two-channel isotropic Kondo model at the Emery-Kivelson line [compare Eq. (23) with $J_y = 0$]. The impurity correction to the ground-state energy can again be obtained from the Green's function. The propagator for the impurity has exactly the form Eq. (24) with Γ_k replaced by

$$\Gamma = \frac{J_0^2 |r|^2}{4\pi a v_F} = \Gamma_a + \Gamma_b. \quad (38)$$

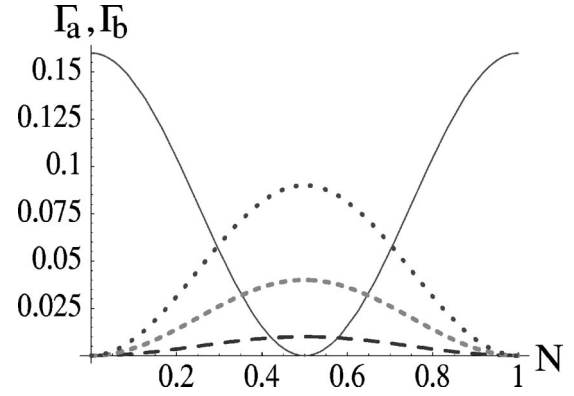


FIG. 3. The resonance energies Γ_a and Γ_b of Eq. (25) are shown. The parameter $|R|$ in Γ_b (solid line) is $|R|=0.4$. The size of the resonance Γ_a grows with increasing anisotropy and thus with increasing $|\delta r|$. The long-dashed line in the graph corresponds to $|\delta r|=0.1$, the short-dashed line to $|\delta r|=0.2$, and the dotted line to $|\delta r|=0.3$. The energies are measured in units of $E_C \gamma / \pi$.

The second equation can be verified by explicit calculation of the sum of the two resonance energies given in Eq. (25). The impurity correction can be found from Eq. (26) in the channel-symmetric limit. Furthermore, the density of states of the impurity was defined in Eq. (27). Combining these expressions we find for the impurity energy

$$\delta\epsilon = -\frac{\Gamma}{2\pi} \ln\left(\frac{E_C^2 + \Gamma^2}{2\Gamma^2}\right) \approx -\frac{\Gamma}{\pi} \ln\left(\frac{E_C}{\Gamma}\right). \quad (39)$$

In the second equation we have used $\Gamma \ll E_C$. It is now clear that the use of the two-channel anisotropic model is justified whenever $\max\{\Gamma_a, \Gamma_b\} \approx \Gamma_a + \Gamma_b$. This condition is certainly met when N is very close either to an integer or to a half-integer value. Furthermore, the range of N values for which the equation is approximately true will be larger for stronger asymmetry between Γ_a and Γ_b , i.e., for a weak asymmetry between the reflection amplitudes $|r_1|$ and $|r_2|$.

In the two cases of electrons with spin in zero magnetic field or with a weak magnetic field we have $\max(\Gamma_a) \ll \max(\Gamma_b)$ and the channel-anisotropic Kondo model is more convenient (See Fig. 3): In particular, the asymmetry simply produces a new energy scale obviously affecting the properties of the system close to the degeneracy point $N = 1/2$. This also allows to make explicit links with the small transmission limit (see Sec. VII).

B. Applications

We will now discuss a case for which the isotropic model is particularly well suited. This is the case of strong asymmetry between the reflection amplitudes of the two transmitted channels. We assume that one of the two channels is very close to perfect transmission, e.g., $|r_1| \rightarrow 0$ and $|r_1| \ll |r_2| \ll 1$. Such a situation can be reached in a strong magnetic field where the electrons are essentially spin polarized. The number of open channels and their reflection amplitudes can then be adjusted by changing the voltage applied to the gates used to define the QPC. The wave functions for the electrons

in the two channels are $\Psi_{\alpha=1} = \Psi_{\uparrow(1)}^{n=1}$ and $\Psi_{\alpha=2} = \Psi_{\uparrow(1)}^{n=2}$. In the limit of interest here the energy $\delta\epsilon$ with the help of Eqs. (38) and (39) is found to be

$$\delta\epsilon = \frac{\gamma E_C}{\pi^2} |r_2|^2 [1 + 2\lambda \cos(2\pi N)] \times \ln\{(\gamma |r_2|^2 / \pi)(1 + 2\lambda \cos(2\pi N))\}, \quad (40)$$

where $\lambda = |r_1|/|r_2|$ is a small parameter. To leading order in λ the correction to the capacitance is given by

$$\delta C = +8\gamma E_C \beta^2 |r_1| |r_2| \ln(|r_2|^2) \cos(2\pi N). \quad (41)$$

First we observe that at perfect transmission $|r_1|=0$ there is no signature of Coulomb blockade left as it is expected.^{8,5,13,28} Furthermore, it is interesting to notice that with one channel very close to perfect transmission the Coulomb-blockade oscillations are strongly reminiscent of the one-channel case, also discussed in Ref. 9.

V. RENORMALIZATION-GROUP FORMULATION

We will now show that the energy scales Γ_a and Γ_b can also be found from a renormalization-group treatment. To do this we will use a similar argument as was put forward in Ref. 13 which in turn is based on Ref. 29. We will first discuss the channel symmetric case $|r_1|=|r_2|$ (electrons with spin and zero magnetic field). The backscattering Hamiltonian for this case is given by

$$H_{bs} = \frac{2|r_1|}{\pi a} \sqrt{\gamma E_C v_F} \cos(\pi N) \cos[\sqrt{2\pi} \phi_s(0)]. \quad (42)$$

The basic idea of the renormalization-group treatment applied here is to calculate the partition function to second order in the small parameter $|r_1|$ and to choose $|r_1|$ as a function of the lattice step a in such a way that the partition function remains invariant under the transformation $a \rightarrow a' = a \exp(l)$. The correction to the partition function due to the backscattering perturbation is

$$\begin{aligned} \delta Z &= - \int_0^\beta d\tau_1 d\tau_2 \langle H_{bs}(\tau_1) H_{bs}(\tau_2) \rangle \\ &= - \frac{J_x^2}{(2\pi a)^2} \int_0^\beta d\tau_1 d\tau_2 \frac{a}{v_F |\tau_1 - \tau_2|}. \end{aligned} \quad (43)$$

Using the definition of J_x given in Eq. (19) it can be seen that the partition function δZ is independent of the lattice step a and thus $|r_1|$ is invariant under rescaling. We now introduce a *dimensionless* parameter $|\tilde{r}_1|$ via $|\tilde{r}_1| = J_x / v_F$. With the help of this parameter we can rewrite the backscattering Hamiltonian in the standard form

$$H_{bs} = \frac{v_F |\tilde{r}_1|}{2\pi a} \cos[\sqrt{2\pi} \phi_s(0)]. \quad (44)$$

From this we can see that $|\tilde{r}_1| = 4|r_1| \sqrt{\gamma E_C a / v_F} \cos(\pi N)$ has the meaning of an effective reflection amplitude. Since $|\tilde{r}_1|$

$\propto \sqrt{a}|r_1|$ it is clear that $|\tilde{r}_1|$ grows under the renormalization $a \rightarrow a' = a \exp(l)$. The renormalization flow equation for $|\tilde{r}_1|$ is given by

$$\frac{d}{dl} |\tilde{r}_1(l)| = \frac{1}{2} |\tilde{r}_1(l)|. \quad (45)$$

We can now integrate this equation from $l=0$ ($a'=a$) to $l=l_c$ [$a'=a_c = a \exp(l_c)$], where a_c is the value of a' for which $J_x \propto |\tilde{r}_1|$ departs to strong coupling, that is, $|\tilde{r}_1(a')| \sim 1$. Integrating we get $|\tilde{r}_1(a_c)|^2 = (a_c/a) |\tilde{r}_1(a)|^2 = 1$. The corresponding critical energy scale is defined through

$$E_{x,c} \approx v_F / a_c = v_F |\tilde{r}_1(a)|^2 / a = J_x^2 / (a v_F). \quad (46)$$

Comparing Eq. (46) to Eq. (25) we see that $E_{x,c}$ is equal to Γ_b up to a numerical factor. Further evaluation of Eq. (46) gives

$$E_{x,c} = 16|r_1|^2 \gamma E_C a \cos^2(\pi N). \quad (47)$$

Similar considerations can be used in the more general case where $|r_1| \neq |r_2|$. Then we have to use, e.g., the backscattering Hamiltonian Eq. (16) as a starting point. Expanding the partition function to the second order in this perturbation (the small parameters are $|R| = |r_1| + |r_2|$ and $|\delta r| = |r_2| - |r_1|$) we get

$$\delta Z = - \frac{J_x^2 + J_y^2}{(2\pi a)^2} \int_0^\beta d\tau_1 d\tau_2 \frac{a}{v_F |\tau_1 - \tau_2|}, \quad (48)$$

where the partition function is again independent of the lattice step a . Furthermore, it is important to note that terms proportional to J_x and J_y do not mix in the expansion of the partition function up to second order.

For a small channel anisotropy, either the coupling J_x or J_y grows under renormalization, which gives rise to two *independent* energy scales. The critical energy for which J_x (J_y) departs to strong coupling is $E_{x,c} = J_x^2 / (v_F a) \propto E_C |R|^2 \cos^2(\pi N)$ [$E_{y,c} = J_y^2 / (v_F a) \propto |\delta r|^2 E_C \sin^2(\pi N)$]. Of course we have recovered here, up to a numerical factor the two energies $\Gamma_a (\propto E_{y,c})$ and $\Gamma_b (\propto E_{x,c})$ [see Eq. (25)]. More generally, using Eq. (48) we find:

$$\frac{d}{dl} [|\tilde{R}(l)|^2 + |\tilde{\delta r}(l)|^2] = [|\tilde{R}(l)|^2 + |\tilde{\delta r}(l)|^2], \quad (49)$$

where we defined $|\tilde{R}| = J_x / v_F$ and $|\tilde{\delta r}| = J_y / v_F$. In the case of a strong channel anisotropy, we deduce that the effective coupling $J_x^2 + J_y^2$ flows off to strong coupling at the critical energy $E_c = (E_{x,c} + E_{y,c})$. Again, we recover $E_c \propto \Gamma = \Gamma_b + \Gamma_a$. For a small anisotropy, of course this reduces to $E_c \propto \max\{\Gamma_a, \Gamma_b\}$.

VI. REALIZATION IN A TWO-CONTACT SETUP

Let us now briefly emphasize that the channel-anisotropic two-channel Kondo model of Sec. III is also well suited to discuss the conductance behavior of a two-contact setup à la Furusaki-Matveev. In this setup, which is a natural extension

of the geometry shown in Fig. 1, a single dot is coupled to two different electron reservoirs via two point contacts. A back gate or side gate is used to vary the Coulomb energy. The device is illustrated in Ref. 17.

Let us start with a strong magnetic field such that the electrons of each reservoir are fully polarized. We obtain an effective two-channel model where $\alpha=1(2)$ now denotes the electrons of the left (right) QPC. Again, we are mainly interested in the case of a *small channel anisotropy* where reflection amplitudes at each contact, namely, $|r_1|$ and $|r_2|$, are close to each other: $|r_1| < |r_2| \ll 1$. It is convenient to associate the centers of the two constrictions with the point $x=0$, meaning that electrons in the dot are described by $\Psi_{1,L(R)}$ at $x>0$ and by $\Psi_{2,L(R)}$ at $x<0$.¹⁷ We introduce the variables ϕ_t and ϕ_c via

$$\phi_1 = \frac{1}{\sqrt{2}}(\phi_t + \phi_c), \quad \phi_2 = \frac{1}{\sqrt{2}}(\phi_t - \phi_c), \quad (50)$$

and similarly for θ_1 and θ_2 . Typically, here ϕ_c is the bosonic variable associated to the *charge* in the dot, while ϕ_t is the one related to the *current* passing through the dot. The main difference with the one-contact setup is that here the charge on the dot rather reads (note the minus sign)¹⁷

$$Q = \frac{1}{\sqrt{\pi}}[\phi_1(0) - \phi_2(0)]. \quad (51)$$

It is straightforward to show that the backscattering Hamiltonian is of the form of Eq. (16) or Eq. (18) with ϕ_s replaced by ϕ_t , explicitly

$$H_{bs} = \frac{J_x}{\pi a} \cos[\sqrt{2\pi}\phi_t(0)]\hat{S}_x + \frac{J_y}{\pi a} \sin[\sqrt{2\pi}\phi_t(0)]\hat{S}_y. \quad (52)$$

The Kondo parameters are given in Eq. (19) where $|\delta r| \ll |R| \ll 1$, and the kinetic energy for the symmetric charge mode $H_{Kin}(\phi_t, \theta_t)$ is still of the form of Eq. (8). Again, we insist on the fact that this mapping is more intuitive than the one of Eq. (17) because the anisotropy of the reflection coefficients is directly related to the anisotropy between coupling parameters in the Kondo model. In consequence, we have two independent energy scales Γ_a and Γ_b . The behavior of the conductance close to the degeneracy point $N = 1/2$ becomes really transparent.

In the absence of any backscattering, the system is equivalent to two resistances $2\pi\hbar/e^2$ (those of the two QPCs) connected in series. Therefore, the conductance is $G_0 = e^2/(4\pi\hbar)$. This is in fact still the case for *finite* barriers in the symmetric case $|r_1| = |r_2|$ at the degeneracy point,³⁰ where both J_x and J_y are zero for $N=1/2$. As was found in Ref. 17 the conductance is still at its resonant value G_0 and the tails of the peak at $N=1/2$ are not Lorentzian: $G \propto (N - 1/2)^{-4}$ due to the J_x coupling. When $|\delta r|$ is finite, from Eq. (52) we immediately see that the asymmetry between channels engenders a finite backscattering process at $N = 1/2$ (again, $J_y \propto |\delta r|$):

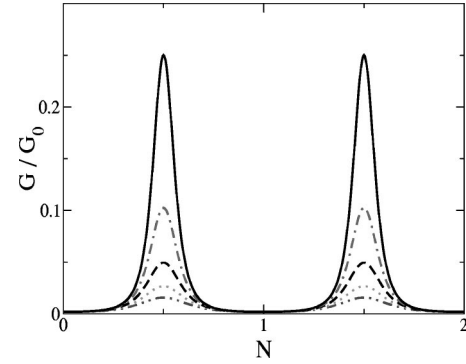


FIG. 4. Conductance in the two-contact setup as a function of N for different values of the (small) anisotropy parameter $|\delta r| = |r_2| - |r_1|$. The parameter $|R| = |r_1| + |r_2|$ is here set to $|R| = 7/10$. The different curves have been calculated for $T/E_c = 1/50$ and have been normalized to G_0 . In order of decreasing conductance peak height the different curves here correspond to $|\delta r| = 0.2$ (top), $|\delta r| = 0.25$, $|\delta r| = 0.3$, $|\delta r| = 0.35$, and $|\delta r| = 0.4$ (bottom).

$$\begin{aligned} H_{bs} &= \frac{J_y}{\pi a} \sin[\sqrt{2\pi}\phi_t(0)]\hat{S}_y, \\ &= \frac{J_y}{\sqrt{4\pi a}}[\psi(0) - \psi^\dagger(0)]a. \end{aligned} \quad (53)$$

This produces the same physics as a nonmagnetic impurity in a Luttinger liquid with the Luttinger exponent being $g = 1/2$.²⁹ The problem becomes exactly solvable using the fermionization procedure of Appendix A. In particular, the current through the device takes the required form:²⁵

$$I = e v_F \psi^\dagger(0) \psi(0). \quad (54)$$

For temperatures $T \ll E_{y,c}$ and N close to $1/2$, the effective potential scattering J_y (or the asymmetry parameter) *diverges* and the conductance then obeys:²⁵

$$G(T; N \approx 1/2) = G_0 \left(\frac{T}{E_{y,c}} \right)^{2/g-2} \propto \left(\frac{T}{E_c N^2} \right)^2, \quad (55)$$

where the second equation is true for $g = 1/2$. The energy $E_{y,c}$ was defined in the last paragraph of the preceding section. For nonsymmetric barriers the conductance peak height (like the capacitance peak height before) becomes strongly dependent on the finite asymmetry between reflection amplitudes at the QPCs (Fig. 4). This naturally reflects the fact that the on-resonance behavior of the system for $N = 1/2$ is very different if the two barriers are not identical.

A simple explanation can be given using the channel-anisotropic two-channel Kondo model. On resonance, the small asymmetry inevitably grows under renormalization. At low temperatures $T \ll \max\{\Gamma_a, \Gamma_b\}$, the conductance behavior for all values of N is given by

$$G(T; N) = G_0 \left(\frac{T}{\max\{\Gamma_a, \Gamma_b\}} \right)^2 \ll G_0. \quad (56)$$

This can also be rewritten as¹⁷

$$G(T;N) \propto \left(\frac{T}{\Gamma}\right)^2, \quad (57)$$

where [see Eq. (38)]

$$\Gamma \propto [|r_1|^2 + |r_2|^2 + 2|r_1||r_2|\cos(2\pi N)], \quad (58)$$

even though this formula seems a little bit less intuitive. In particular, the N dependence of the conductance for $N \approx 1/2$ is less apparent. It is worth noting that the quadratic temperature dependence is a universal property of inelastic cotunneling. But, close to $N=1/2$ this can also be interpreted as a nice manifestation of the restoration of the *Fermi-liquid* behavior due to the finite asymmetry between channels (like for the capacitance problem).

Unfortunately, the present approach does not allow a complete solution for the case of fermions with spin in the two-contact setup.¹⁷ At zero magnetic field and for completely symmetric barriers at the two QPCs, there exists a mapping onto a four-channel Kondo model for the Hamiltonian (which could help to compute thermodynamical properties), but it is very difficult to rigorously compute current-current correlation functions in the new basis and then to extract the conductance behavior. The current operator indeed exhibits an unusual form as indicated in Appendix B of Ref. 17. Therefore, the height of the conductance peak cannot be calculated in a rigorous manner even for completely symmetric barriers at zero temperature. Furthermore, the mapping onto the Kondo problem is only valid at (close to) $N=1/2$. To extend the (four-channel) Kondo mapping to the case of asymmetric barriers remains a challenging task.

VII. SMALL TRANSMISSION LIMIT

Having so far concentrated on the limit where the quantum dot is strongly coupled to a reservoir through a highly transmissive quantum point contact, we will in this section consider the limit of weak coupling. The similarity between the Coulomb-blockade problem in this limit and a Kondo model was noticed by Glazman and Matveev.⁷ An explicit mapping of the Coulomb-blockade Hamiltonian on a Kondo model was used by Matveev to calculate the charge and the capacitance of the quantum dot in the weak transmission limit.⁵ Note that recently a noncrossing approximation has been generalized to this type of multichannel Kondo models.³¹

We will here rederive Matveev's mapping and discuss the straightforward extension of his model to the channel anisotropic case. Again our discussion will be restricted to the case of two transport channels through the point contact. The anisotropy between the transmission amplitudes for the two transport channels in the QPC will still give rise to a mapping on a channel-anisotropic Kondo model; But here, the system flows off to the usual *spin-isotropic* fixed point, i.e., $J_{\sigma,\perp} = J_{\sigma,z} \gg 0$. We will see below that the problem of calculating the average charge $\langle Q \rangle$ on the dot is now equivalent to the problem of finding the average of the z component $\langle S_z \rangle$ of the impurity spin in the Kondo model. In addition, the capacitance of the dot is the same as the magnetic susceptibility χ of the impurity. Once this equivalence is established

the problem is solved, since these quantities ($\langle S_z \rangle$, χ) can be found in the literature. The channel- and spin-*isotropic* multichannel Kondo problem was solved exactly in this limit in Refs. 32,33, while the impurity susceptibility for the *channel-anisotropic* (but spin-isotropic) two-channel Kondo problem can be simply extracted from Ref. 34. Note in passing that the channel-anisotropic case was also solved (exactly) using Bethe ansatz in Ref. 35. There, the Wilson ratio is computed even in the case of a channel anisotropy. This model has also been investigated using conformal field theory and numerical renormalization-group calculations in Ref. 36.

We will now proceed to writing down the model for our system in the small transmission limit. Instead of formulating it in momentum space as it was done by Matveev we will here use a real-space formulation that allows us to stress the analogy with the corresponding model in the strong transmission limit (see Sec. II). In Appendix C, we will also address the question why the mapping on the Kondo model cannot be derived using bosonization as it was done in Sec. III. In the preceding section we have treated the backscattering as a small perturbation to an otherwise perfectly transparent QPC. In this section the perturbation is a tunneling Hamiltonian that couples two *a priori* independent systems (the 2DEG and the dot). A smooth transition can be made from the strongly to the weakly coupled limit by continuously increasing the auxiliary gate voltage to pinch off the QPC. In this transition a perfectly transmissive one-dimensional channel n will be cut into two weakly coupled halves. In the vicinity of the center of the QPC electron motion is still quasi-one-dimensional. Electronic wave functions to the left of the center of the QPC (in the reservoir) will be denoted $\Psi_{\sigma,0}^n$, wave functions to the right of the center [in the quantum dot (QD)] are $\Psi_{\sigma,1}^n$. Again σ is the spin index, n the channel index due to lateral confinement, and here $\alpha=0,1$ indicates the location of the electron. Hopping between the two sides of the QPC constitutes a small perturbation. To model this perturbation we use the Hamiltonian

$$H_T = \sum_{\sigma=1,2} [|t_\sigma| \Psi_{\sigma,1}^\dagger(0) \Psi_{\sigma,0}(0) + \text{H.c.}]. \quad (59)$$

Note that the kinetic energies $H_{kin}^0(\{\Psi_{\sigma,0}^\dagger, \Psi_{\sigma,0}\})$ and $H_{kin}^1(\{\Psi_{\sigma,1}^\dagger, \Psi_{\sigma,1}\})$ for electrons in the 2DEG and the dot have the form of Eq. (22). The boundaries for the integration along the x axis are $-\infty, 0$ in H_{kin}^0 and $0, \infty$ in H_{kin}^1 . The Coulomb interaction can be modeled as in Sec. II, Eq. (3) the charge on the dot being

$$Q = \int_0^\infty dx [\Psi_{\sigma,1}^\dagger(x) \Psi_{\sigma,1}(x) - \rho_0]. \quad (60)$$

The equilibrium charge density ρ_0 is chosen in such a way that the total charge Q on the dot is zero when no voltage is applied to the gate ($V_G=0$).

We now want to concentrate on the point $N=1/2$ where the states with $Q=0$ and $Q=1$ are energy degenerate [see Eq. (3)], and therefore charge fluctuations are large. We in-

roduce the small parameter $U = e/(2C_{gd}) - V_G \propto (N - 1/2)$ to measure deviations of N from the degeneracy point. In terms of U the electrostatic energies of the two states $Q = 0$ and $Q = 1$ are $E_0 = 0$ and $E_1 = eU$, respectively.

If the two conditions $|U| \ll e/C_{gd}$ and $kT \ll E_C$ are met only the two states with $Q = 0$ and $Q = 1$ are accessible and higher-energy states can be removed from our theory introducing the projection operators P_0 and P_1 . Here P_0 and P_1 are projecting on the states $Q = 0$ and $Q = 1$, respectively. The effective Hamiltonian for this truncated system is

$$H_{eff} = (H_{kin}^0 + H_{kin}^1)(P_0 + P_1) + eUP_1 + \sum_{\sigma=1,2} (|t_\sigma| \Psi_{\sigma,1}^\dagger \Psi_{\sigma,0} P_0 + |t_\sigma| \Psi_{\sigma,0}^\dagger \Psi_{\sigma,1} P_1), \quad (61)$$

where the operators in the tunneling part are evaluated at $x = 0$ [see Eq. 59]. From this equation we see that $\partial H / \partial U = eP_1$ and therefore $\langle Q \rangle = \partial E_0 / \partial U$ where E_0 is the ground-state energy of the Hamiltonian Eq. (61). It can be shown that the Hamiltonian Eq. (61) is equivalent to the Hamiltonian

$$H_K = \sum_{\alpha=0,1} H_{kin}^\alpha + 2hS_z + \frac{1}{2} \sum_{\sigma=1,2} \{J_{\sigma,\perp} [s_\sigma^+(0)S^- + s_\sigma^-(0)S^+]\}, \quad (62)$$

which has the form of a standard Kondo Hamiltonian. The equivalence between the Hamiltonians Eq. (61) and Eq. (62) was demonstrated by Matveev in Ref. 9. For completeness we rederive this relation in Appendix C taking channel anisotropy into account explicitly. In Eq. (62) we have introduced the transversal Kondo coupling parameters $J_{\sigma,\perp} = 2|t_\sigma|$ and an effective external magnetic field $h = eU/2 \propto (N - 1/2)$ applied along the z axis. Note that Eq. (62) corresponds to the limit $J_{1,z} = J_{2,z} = 0$ of Eq. (1). We have dropped the constant $eU/2$ from the Hamiltonian in Eq. (62). Therefore, the ground-state energy $E_{K,0}$ of the Kondo Hamiltonian Eq. (62) is related to the ground-state energy E_0 of the effective Hamiltonian Eq. (61) through $E_{K,0} + eU/2 = E_0$. Since $2\langle S_z \rangle = \partial E_{K,0} / \partial h$ and $\langle Q \rangle = \partial E_0 / \partial U$ we are led to the obvious identification

$$\langle Q \rangle = e \left(\frac{1}{2} + \langle S_z \rangle \right). \quad (63)$$

Combining Eq. (5) with $U = e/(2C_{gd}) - V_G$ we find for the correction to the capacitance $C = -\partial \langle Q \rangle / \partial U \propto \chi = \partial \langle S_z \rangle / \partial h$, where χ is the impurity susceptibility (Since h only acts on S_z , χ is also equivalent to the local magnetic susceptibility χ_l).

So we have now shown that a calculation of the capacitance of the quantum dot coupled to a 2DEG through a QPC with two transport channels with *different* transmission amplitudes is equivalent to a calculation of the impurity susceptibility in the channel-anisotropic two-channel Kondo model. It is known that both $J_{\sigma,z} = 0$ and $J_{\sigma,\perp} \ll 1$ grow under renormalization and that for small enough energies $J_{\sigma,z} = J_{\sigma,\perp}$

$= J_{\sigma,\perp} |t_\sigma|$ even if we start from a spin-anisotropic Kondo model. The resulting spin-isotropic Kondo model was solved in Refs. 32 and 33. In the zero-temperature limit the impurity susceptibilities for the one-channel case and the two-channel isotropic limit are

$$\chi \propto \begin{cases} \text{const}, & J_2 = 0, \\ \ln h, & J_1 = J_2. \end{cases} \quad (64)$$

Note that the susceptibility for the two-channel case diverges in the zero magnetic field limit. The channel-anisotropic (but spin-isotropic) Kondo model was discussed, e.g., by Coleman and Schofield³⁴ (also by Andrei and Jerez³⁵ and by Affleck *et al.*³⁶) who found for the susceptibility at zero magnetic field ($h = 0$),

$$\chi \propto 1 - \frac{\ln(\nu)}{\nu - 1}, \quad (65)$$

where the anisotropy parameter $\nu \propto |\delta t| / T$ with $|\delta t| \propto |J_1 - J_2|$ and $T \propto (J_1 + J_2)$, is $\nu = 1$ in the one-channel limit ($J_2 = 0$) and $\nu = 0$ in the two-channel isotropic limit. Equation (65) thus reproduces correctly the main characteristics of the result Eq. (64) in these two limiting situations. From the results for the susceptibility we immediately obtain the capacitance

$$\delta C \propto \begin{cases} \text{const}, & J_2 = 0, \\ \ln(N - 1/2), & J_1 = J_2, \\ \ln|\delta t|, & J_1 \neq J_2, \quad N = 1/2. \end{cases} \quad (66)$$

The results for the one-channel and the two-channel isotropic cases are due to Matveev.⁹ The main observation we want to make here is that a small channel anisotropy cuts off the logarithmic divergence exactly in the same way as in the case discussed in the previous sections where the reflection amplitudes in the QPC could be treated as small parameters.

VIII. CONCLUSIONS

We have applied the channel- (and spin-) anisotropic two-channel Kondo model to study Coulomb-blockade oscillations in the capacitance of a quantum dot. Our main interest has been to investigate the effect of an asymmetry between the reflection (or transmission) amplitudes of different open channels in the QPC connecting the dot to a reservoir. Following Matveev^{5,9} we have studied the two exactly soluble limits of very weak ($|t_1|, |t_2| \ll 1$) and very strong coupling ($|r_1|, |r_2| \ll 1$). A summary of the results for the capacitance in different limits is given in Table I.

In both limits a mapping of the original problem onto a Kondo model is possible. Remember that these results concern the limit of very low temperature where quantum fluctuations are prominent. At quite high temperature, the Kondo physics gets destroyed by thermal fluctuations.^{9,13,22}

For weak backscattering at the point contact ($|r_1|, |r_2| \ll 1$) the original problem can be mapped¹⁴ on a channel anisotropic Kondo model at the Emery-Kivelson¹⁰ line ($J_{1,z} = J_{2,z} = 2\pi v_F$). For this particular value of the coupling constant the Kondo model is exactly solvable. The anisotropy of

TABLE I. We have listed here all the results for the capacitance of the quantum dot at $N \rightarrow 1/2$ and the respective references. The divergence occurring at $N \rightarrow 1/2$ in the channel-isotropic *two*-channel limit is cut off by a channel anisotropy for both weak and strong reflection at the QPC.

No. of channels	Reflection or transmission coefficient	Capacitance at $N=1/2$	Ref.
1	$ r_1 \ll 1, (r_2 \rightarrow 1)$	constant	Ref. 9
2	$ r_1 = r_2 \ll 1$	$-\ln N-1/2 $	Ref. 9
2	$ r_1 \neq r_2 \ll 1$	$-\ln(r_2 - r_1)$	Ref. 14, Secs. III-V
1	$ t_1 \ll 1, (t_2 \rightarrow 0)$	constant	Ref. 5
2	$ t_1 = t_2 \ll 1$	$-\ln N-1/2 $	Ref. 5
2	$ t_1 \neq t_2 \ll 1$	$-\ln(t_1 - t_2)$	Sec. VII

the reflection amplitudes for different channels is directly reflected in the channel anisotropy of the Kondo model. In fact we found $J_{1,\perp} \propto |r_1|$ and $J_{2,\perp} \propto |r_2|$, where $J_{1,\perp}$ and $J_{2,\perp}$ are the coupling constants for the two channels in the Kondo model. The mapping allowed us to calculate the shift of the ground-state energy of our Hamiltonian due to the back-scattering at the point contact and in turn to find the capacitance of the quantum dot. While the capacitance is logarithmically divergent for values of the gate voltage close to $N = n + 1/2$ (n is an integer) in the isotropic limit⁹ ($|r_1| = |r_2|$), this divergence is *cut off* by a small anisotropy between the reflection amplitudes of different channels.¹⁴ *This can be interpreted as a manifestation of the restoration of the Fermi-liquid behavior close to the degeneracy points $N = n + 1/2$ due to the asymmetry between channels.*

Note that a similar conclusion can be reached investigating the conductance behavior in a two-contact setup in a strong magnetic field where $|r_1|$ and $|r_2|$ denote the back-scattering amplitudes at the two different point contacts. The on-resonance behavior ($G = G_0 = e^2/2h$) for $N = 1/2$ is *reduced* for a small anisotropy between $|r_1|$ and $|r_2|$.

There are two intrinsic energy scales [$\Gamma_b \propto (|r_1| + |r_2|)^2$ and $\Gamma_a \propto (|r_1| - |r_2|)^2$] in the channel-anisotropic Kondo model. Each can be interpreted as the resonance energy related to coupling half an impurity to the conduction electrons. In the channel-isotropic case only half the impurity spin is screened by the conduction electrons. Coupling back the second half of the impurity to the conduction electrons leads to the emergence of a second energy scale Γ_a . It is this new energy scale that enters the expression for the capacitance and cuts off the divergence at $N = n + 1/2$. Unfortunately there is no direct correspondence between the magnetic susceptibility in the Kondo model and the capacitance of the quantum dot. Such an equivalence exists only in the limit of small transmission. It is true, however, that the behavior of the capacitance (found from the Kondo model at the Emery-Kivelson line) is reminiscent of the impurity susceptibility $\chi = \partial^2(\delta\epsilon)/\partial h^2$ away from the Emery-Kivelson line or of the local magnetic susceptibility $\chi_l = \partial(\hat{S}_z)/\partial h$ at the Emery-Kivelson line.

In this paper we have extended our previous work¹⁴ deriving the mapping on the anisotropic Kondo model in a pedagogical way and carefully discussing its limits of validity. We have then given an alternative way for calculating the

charge on the quantum dot using a mapping¹⁷ on a channel-isotropic two-channel Kondo model. In this approach, the coupling constant is a complex parameter depending on both $|r_1|$ and $|r_2|$. While the latter approach has the advantage of being exact, it seems less intuitive since the anisotropy of the reflection coefficients is not directly reflected as an anisotropy between coupling parameters in the Kondo model. We have in addition used a simple scaling argument to recover the intrinsic energy scales Γ_a and Γ_b that occur in the expression of the capacitance.

We relied on purely mathematical arguments to show the equivalence between the Coulomb-blockade problem and the Kondo Hamiltonian in the strong tunneling limit ($|r_1|, |r_2| \ll 1$). In the opposite limit $|t_1|, |t_2| \ll 1$ the similarity of these two problems can be understood using a comparably simple physical argument (see Ref. 9 and Appendix C). The main observation is that at low enough temperatures $T \ll E_C$ and for voltages close to $N = n + 1/2$ only two charge states on the quantum dot are energetically accessible (e.g., $Q = 0, Q = 1$). The charge state of the dot is then interpreted as a pseudo-spin-1/2 degree of freedom, which corresponds to the impurity spin in the Kondo model. The real spin of the conduction electrons in the Kondo model is replaced by an index α indicating the location of an electron (distinguishing between electrons to the left and to the right of the QPC) in the Coulomb-blockade problem.

A first-order process in the Kondo problem that flips the impurity spin from up to down and the spin of a conduction electron from down to up is then equivalent to a tunneling process that takes an electron from the left to the right and changes the charge on the dot from $Q = 0$ to $Q = 1$. The Kondo coupling parameters simply are $J_{1(2),\perp} \propto |t_{1(2)}|$ and $J_{1(2),z} = 0$. As it is clear from the derivation of the mapping there exists an equivalence between the charge on the dot and the impurity spin, namely, $\langle Q \rangle \propto \langle S_z \rangle$. It was furthermore shown that the capacitance is basically the same (up to some constant) as the impurity susceptibility. Since the model with $J_{1(2),\perp} \propto |t_{1(2)}|$ and $J_{1(2),z} = 0$ flows to the usual spin-isotropic fixed point we have been able to use the known result for the impurity susceptibility in the channel-anisotropic two-channel Kondo model with $J_{\sigma,\perp} = J_{\sigma,z} \gg 0$,³⁴ to discuss the effect of channel anisotropy on the capacitance. Exactly as in the limit of strong transmission the capacitance diverges in the channel-isotropic case,⁵ but the di-

vergence is cut by the anisotropy. Note that no immediate connection can be made with the Kondo model at the Emery-Kivelson line ($J_{1(2),z} = 2\pi v_F$), which we obtained when treating the small reflection limit.

All the results on the behavior of the capacitance of the dot close to $N = 1/2$ are summarized in Table I.

ACKNOWLEDGMENT

This work was supported by the Swiss National Science Foundation.

APPENDIX A: REFERMIONIZATION

In this Appendix we want to elaborate on the unusual refermionization procedure that we used in Sec. III. The backscattering part of the bosonic Hamiltonian to be refermionized is given in Eq. (18). The kinetic energy is of the form

$$H_{Kin} = v_F \int_{-\infty}^{\infty} dx \{ [\partial_x \phi_s(x)]^2 + \pi_s(x)^2 \}. \quad (A1)$$

It will turn out to be convenient to use the field $\pi_s(x)$ instead of $\theta_s(x)$ for the moment. The two fields are related through $\pi_s(x) = \partial_x \theta_s(x)$. The commutation relations for the fields $\phi_s(x)$ and $\pi_s(x)$ are $[\phi_s(x), \pi_s(y)] = i\delta(x-y)$, $[\phi_s(x), \phi_s(y)] = 0$, and $[\pi_s(x), \pi_s(y)] = 0$. The basic idea of the refermionization procedure is to introduce an operator $\psi(x)$ such that $\cos[\sqrt{2\pi}\phi_s(0)] \propto \psi(0) + \psi^\dagger(0)$ and $\sin[\sqrt{2\pi}\phi_s(0)] \propto \psi(0) - \psi^\dagger(0)$. It is clear that for such an operator

$$\psi(0) = \frac{1}{\sqrt{2\pi a}} \exp[i\sqrt{2\pi}\phi_s(0)]. \quad (A2)$$

In addition the operator must obey the usual fermionic anti-commutation relations. Using the relation $e^A e^B = e^B e^A e^{[A,B]}$ it can be seen that the obvious choice for ψ , namely, $\psi(x) = (2\pi a)^{-1/2} \exp[i\sqrt{2\pi}\phi_s(x)]$ does not obey anticommution relations. To construct a fermionic operator we introduce the auxiliary fields

$$\begin{aligned} \phi_\pm(x) &= \frac{1}{\sqrt{2}} [\phi_s(x) \pm \phi_s(-x)], \\ \pi_\pm(x) &= \frac{1}{\sqrt{2}} [\pi_s(x) \pm \pi_s(-x)]. \end{aligned} \quad (A3)$$

In terms of these new fields the kinetic energy is

$$H_{Kin} = v_F \sum_{\alpha=\pm} \int_0^\infty dx [(\partial_x \phi_\alpha)^2 + (\partial_x \theta_\alpha)^2]. \quad (A4)$$

We thus arrive at a theory that is confined to positive values of x . The advantage of this restriction becomes clear when we introduce the two additional right-going and left-going fields

$$\begin{aligned} \Phi_{R,\pm}(x) &= \phi_\pm(x) - \int_0^x dy \pi_\pm(y), \\ \Phi_{L,\pm}(x) &= \phi_\pm(x) + \int_0^x dy \pi_\pm(y). \end{aligned} \quad (A5)$$

At $x=0$ we have $\Phi_{R,+}(0) = \Phi_{L,+}(0) = \sqrt{2}\phi_s(0)$ and also $\Phi_{R,-}(0) = \Phi_{L,-}(0) = 0$, which makes these fields candidates for the construction of our new fermions. The backscattering Hamiltonian can be expressed through the fields $\Phi_{R,+}(x)$ and $\Phi_{L,+}(x)$ only. There are in fact many ways in which this can be done. However, we will soon get rid of this ambiguity. The fields $\Phi_{R(L),-}(x)$ occur only in the kinetic part of the Hamiltonian and are thus of little interest to us. Later on we will need the commutation relations

$$\begin{aligned} [\Phi_{R,+}(x), \Phi_{R,+}(y)] &= +i \operatorname{sgn}(x-y), \\ [\Phi_{L,+}(x), \Phi_{L,+}(y)] &= -i \operatorname{sgn}(x-y). \end{aligned} \quad (A6)$$

For completeness we also give the correlation functions $G_{R(L)} = \langle \Phi_{R(L),+}(x) \Phi_{R(L),+}(0) - \Phi_{R(L),+}(0)^2 \rangle$, which take the standard form

$$G_{R(L)} = \frac{1}{\pi} \ln \left(\frac{a}{a \pm ix} \right). \quad (A7)$$

The plus sign belongs to the label R while the minus sign belongs to L . The kinetic energy in terms of these new fields takes the form

$$H_{Kin} = \frac{v_F}{2} \sum_{\alpha=\pm} \int_0^\infty dx [(\partial_x \Phi_{R,\alpha})^2 + (\partial_x \Phi_{L,\alpha})^2]. \quad (A8)$$

We now drop the $\Phi_{R(L),-}(x)$ part of the kinetic energy since it is not coupled to the backscattering term. To refermionize the $\Phi_{R(L),+}(x)$ part we introduce the operators

$$\psi_R(x) = \frac{1}{\sqrt{2\pi a}} e^{i\sqrt{\pi}\Phi_{R,+}(x)}, \quad (A9)$$

$$\psi_L(x) = \frac{1}{\sqrt{2\pi a}} e^{i\sqrt{\pi}\Phi_{L,+}(x)}. \quad (A10)$$

Using the commutation relations for the bosonic fields we can verify that the fields $\psi_{R,\pm}(x)$ and $\psi_{L,\pm}(x)$ really are fermions and obey

$$\psi_{p,+}(x) \psi_{p,+}(y) = -\psi_{p,+}(y) \psi_{p,+}(x), \quad (A11)$$

where $p=R,L$. Note, that for $x=0$ we have $\psi_{L,+}(0) = \psi_{R,+}(0)$ [see Eqs. (A5) and (A9)] and there thus seems to be more than one way to refermionize the backscattering Hamiltonian Eq. (18). To lift this ambiguity we reextend our theory on the full x axis via the definition

$$\psi(x) = \mathcal{P} \begin{cases} \psi_R(x), & x > 0, \\ \psi_L(-x), & x < 0. \end{cases} \quad (A12)$$

In the above definition of the fermion $\psi(x)$ [Eq. (A12)] we have introduced an additional phase factor

$$\mathcal{P} = \exp(i\pi d^\dagger d) = 1 - 2d^\dagger d \quad (\text{A13})$$

to ensure that $\psi(x)$ anticommutes with the spin operators \hat{S}_x and \hat{S}_y written in terms of Majorana fermions d and d^\dagger [cf. Eq. (21)]. The second equality in Eq. (A13) holds because $d^\dagger d = 0, 1$ at zero temperature. In the fermionic operators we have defined above, the kinetic energy finally takes the simple form given in Eq. (22) while the backscattering part of the Hamiltonian is

$$H_{bs} = \frac{J_x}{\sqrt{2\pi a}} (\psi(0) + \psi^\dagger(0)) \mathcal{P} \hat{S}_x - \frac{iJ_y}{\sqrt{2\pi a}} [\psi(0) - \psi^\dagger(0)] \mathcal{P} \hat{S}_y. \quad (\text{A14})$$

Using Eqs. (A13) and (21), together with the commutation relations for the operators d and d^\dagger , we can show that $\mathcal{P} \hat{S}_x = -i\hat{S}_y$ and $\mathcal{P} \hat{S}_y = -i\hat{S}_x$. With these relations we recover Eq. (23).

APPENDIX B: GREEN'S FUNCTIONS

Although this is rather standard material (see, e.g., Ref. 25) we believe that it is useful to give a short derivation of the Green's functions Eq. (24). The Fourier transforms of the impurity Green's functions $G_a(\tau) = -\langle T_\tau a(\tau) a(0) \rangle$ and $G_b(\tau) = -\langle T_\tau b(\tau) b(0) \rangle$ can conveniently be found from the equations of motion. We will here only derive the correlation function for a , the correlator for b can be found along the same lines. The Hamiltonian $H_{EK}^A = H_{Kin} + H_{bs}$ of our system is given in Eqs. (22) and (23). The fields ψ and $d = a + ib$ [see Eq. (21)] obey standard fermionic anticommutation relations. Introducing the Majorana components of the field ψ through $z_1(x, \tau) = [\psi^\dagger(x, \tau) + \psi(x, \tau)]/\sqrt{2}$ and $z_2(x, \tau) = [\psi(x, \tau) - \psi^\dagger(x, \tau)]/(i\sqrt{2})$ we see already from the Hamiltonian in Eq. (23) that a couples only to z_2 . We introduce the additional propagator $G_{z_2 a}(x, \tau) = -\langle T_\tau z_2(x, \tau) a(0) \rangle$. The equations of motion for the two coupled correlators $G_a(\tau)$ and $G_{z_2 a}(x, \tau)$ are

$$\begin{aligned} \partial_\tau G_a(\tau) &= -\delta(\tau) + i \frac{J_y}{\sqrt{2\pi a}} G_{z_2 a}(0, \tau), \\ \partial_\tau G_{z_2 a}(x, \tau) &= +i v_F \partial_x G_{z_2 a}(x, \tau) - i \frac{J_y}{\sqrt{2\pi a}} \delta(x) G_a(\tau). \end{aligned} \quad (\text{B1})$$

To solve these equations it is best to go to Fourier space making use of the relations

$$\begin{aligned} G_a(\tau) &= \frac{1}{\beta} \sum_{\omega_n} e^{-i\omega_n \tau} G_a(\omega_n), \\ G_{z_2 a}(x, \tau) &= \frac{1}{\beta} \sum_{\omega_n} \int \frac{dp}{2\pi} e^{-i\omega_n \tau + ipx} G_{z_2 a}(p, \omega_n), \end{aligned} \quad (\text{B2})$$

where the sum is over the fermionic Matsubara frequencies $\omega_n = (2n+1)\pi/\beta$. To calculate the correlator $G_a(\tau)$ we only need to understand the local physics in $x=0$. The local equations of motion in Fourier space are

$$i\omega_n G_a(\omega_n) = 1 - i \frac{J_y}{\sqrt{2\pi a}} G_{z_2 a}(\omega_n), \quad (\text{B3})$$

$$G_{z_2 a}(\omega_n) = i \frac{J_y}{\sqrt{2\pi a}} G^{(0)}(\omega_n) G_a(\omega_n). \quad (\text{B4})$$

To alleviate the notation we have introduced $G^{(0)}(\omega_n) = -i \text{sgn}(\omega_n)/2v_F$. To find $G^{(0)}(\omega_n)$ we Fourier transform the free electron propagator $G^{(0)}(p, \omega_n) = (i\omega_n - v_F p)^{-1}$ with regard to p and take the limit $x \rightarrow 0$. Furthermore, we have defined $G_{z_2 a}(\omega_n) = G_{z_2 a}(x=0, \omega_n)$.

Substituting Eq. (B4) into Eq. (B3) we can solve for $G_a(\omega_n)$ and obtain

$$G_a(\omega_n) = \frac{1}{i\omega_n + i\Gamma_a \text{sgn}(\omega_n)}. \quad (\text{B5})$$

After an analytic continuation $i\omega_n \rightarrow \omega + i\delta$ we recover Eq. (24).

APPENDIX C: MAPPING TO THE KONDO MODEL IN THE SMALL TRANSMISSION LIMIT

In this Appendix first we want to fill in the gaps between Eq. (61) and the Kondo Hamiltonian Eq. (62). Let us consider the tunneling part of the effective Hamiltonian. The first term takes an electron from the 2DEG and transfers it to the QD, the projection operator P_0 makes sure that the charge on the dot is $Q=0$ before the tunneling takes place. The second term takes an electron from the dot to the lead. In our truncated system this process is allowed only when the charge on the dot is $Q=1$. This restriction is implemented through the operator P_1 . The main goal of the following manipulations will be to show the equivalence of the Hamiltonian Eq. (61) to a Kondo Hamiltonian.

To explicitly account for the charge on the dot we make the replacement $|\Phi\rangle \rightarrow |\Phi\rangle|Q\rangle$. Here $|\Phi\rangle$ is any state of our system with charge Q on the dot. The values of Q are limited to $Q=0, 1$ and the states $|Q\rangle = |0\rangle$ and $|Q\rangle = |1\rangle$ can be considered as the basis of a two-dimensional vector space. However, the product $|\Phi\rangle|Q\rangle$ is no tensor product since the charge of the dot is of course not independent of the system's state. The state $|Q\rangle$ should rather be considered as an auxiliary label to $|\Phi\rangle$. In addition to introducing the label $|Q\rangle$ we make the replacement

$$\begin{aligned} \Psi_{\sigma,1}^\dagger \Psi_{\sigma,0} P_0 &\rightarrow \Psi_{\sigma,1}^\dagger \Psi_{\sigma,0} S^+, \\ \Psi_{\sigma,0}^\dagger \Psi_{\sigma,1} P_1 &\rightarrow \Psi_{\sigma,0}^\dagger \Psi_{\sigma,1} S^- \end{aligned} \quad (\text{C1})$$

in Eq. (61). Here S^+ and S^- are pseudospin ladder operators acting only on the charge part $|Q\rangle$.

Since $S^+|Q=1\rangle = 0$ and $S^-|Q=0\rangle = 0$ these operators ensure in the same way as the projection operators P_0 and P_1

that only transitions between states with $Q=0$ and $Q=1$ take place. In addition the charge Q on the dot is adjusted whenever a tunneling process takes place since $S^+|0\rangle=|1\rangle$ and $S^-|1\rangle=|0\rangle$. We would like to emphasize again that only the combinations of pseudospin ladder operators and hopping operators introduced above are meaningful since $|Q\rangle$ and $|\Phi\rangle$ are not independent.

To get rid of the remaining projection operators in Eq. (61) we rewrite (eUP_1) as $[eU(P_0+P_1)/2 + eU(P_1-P_0)/2]$. We observe that

$$\begin{aligned}(P_1 \pm P_0)|0\rangle &= \pm|0\rangle, \\ (P_1 \pm P_0)|1\rangle &= +|1\rangle.\end{aligned}\quad (\text{C2})$$

This leads us to identify $(P_1 - P_0)$ with $2S_z$ and $(P_1 + P_0)$ with the identity operator on the space spanned by $|0\rangle$ and $|1\rangle$. Here we used that for the z -component S_z of the pseudospin we have $S_z|1\rangle=|1\rangle/2$ and $S_z|0\rangle=-|0\rangle/2$. Gathering all terms we can rewrite the effective Hamiltonian Eq. (61) as

$$\begin{aligned}H_{eff} &= (H_{kin}^0 + H_{kin}^1) + eU(2S_z + 1)/2 \\ &+ \sum_{\sigma=1,2} (|t_{\sigma}| \Psi_{\sigma,1}^{\dagger} \Psi_{\sigma,0} S^+ + |t_{\sigma}| \Psi_{\sigma,0}^{\dagger} \Psi_{\sigma,1} S^-).\end{aligned}\quad (\text{C3})$$

We now introduce an additional pseudospin operator $s_{\sigma}^{\pm}(x)$ via

$$\begin{aligned}s_{\sigma}^+ &= \Psi_{\sigma,0}^{\dagger} \Psi_{\sigma,1}, \\ s_{\sigma}^- &= \Psi_{\sigma,1}^{\dagger} \Psi_{\sigma,0},\end{aligned}\quad (\text{C4})$$

where the matrices $\sigma^{\pm} = \sigma_x \pm i\sigma_y$ are standard combinations of Pauli matrices. It is important to note that these pseu-

dospin operators again have nothing to do with the true spin of the electrons but are related to the location of an electron ($\alpha=0$ for an electron in the 2DEG, $\alpha=1$ for an electron in the QD). Introducing the definition of these pseudospins into Eq. (C3) finally leads us to Eq. (62).

Finally, we want to show that in this limit the bosonization approach does not allow us to precisely build a pseudospin operator describing the dot from the original tunnel Hamiltonian. For simplicity, we restrict the discussion to the case of spinless fermions, i.e., we ignore the spin index σ . The main problem we encounter is that at $x=0$ we have open boundaries, implying that $\Psi_1(0) = \Psi_0(0) = 0$. Introducing right (R) and left (L) movers as in Eq. (6), this is equivalent to write, e.g., for the dot, $\Psi_{1,R}(0) + \Psi_{1,L}(0) = 0$. This has the effect to pin the (charge) fields ϕ_1 and ϕ_0 at $x=0$: $\phi_1(0) = \phi_0(0) = \sqrt{\pi}/2$. Therefore, this provides us

$$\Psi_{\alpha,p}(0) = \frac{\mp i}{\sqrt{2\pi a}} e^{i\sqrt{\pi}\theta_{\alpha}(0)}.\quad (\text{C5})$$

From the form of the tunnel term (which can be rewritten either with $\Psi_{1,R}$ or with $\Psi_{1,L}$) we would be tempted to explicitly build the pseudospin operator in the dot, as³⁷

$$S^+ = \Psi_{1,R/L}^{\dagger}(0),$$

$$S^- = \Psi_{1,R/L}(0),$$

$$S_z = \Psi_{1,R/L}^{\dagger}(0) \Psi_{1,R/L}(0) - 1/2.\quad (\text{C6})$$

However, due to the *open* boundary condition at $x=0$, the fermion operator $\Psi_{1,R/L}$ at $x=0$ now only depends on the superfluid phase θ_1 .²⁹ Then, S^+ would commute with S_z and then \vec{S} would not be a quantum spin object. The only way to proceed in order to recover the (correct) Kondo mapping is to introduce the extra label $|Q\rangle$.

*Email address: klehur@serifos.unige.ch

†Email address: seelig@kalygnos.unige.ch

¹For a short review, see L. Kouwenhoven and L. Glazman, Phys. World **14**, 33 (2001).

²D. Goldhaber-Gordon, H. Shtrikman, D. Mahalu, D. Abusch-Magder, U. Meirav, and M. A. Kastner, Nature (London) **391**, 156 (1998); D. Goldhaber-Gordon, J. Göres, M. A. Kastner, H. Shtrikman, D. Mahalu, and U. Meirav, Phys. Rev. Lett. **81**, 5225 (1998).

³S. M. Cronenwett, T. H. Oosterkamp, and L. P. Kouwenhoven, Science **281**, 540 (2001).

⁴For a review, see D. L. Cox and A. Zawadowski, Adv. Phys. **47**, 599 (1998).

⁵K. A. Matveev, Zh. Éksp. Teor. Fiz. **98**, 1598 (1990) [Sov. Phys. JETP **72**, 892 (1991)].

⁶Ph. Nozières and A. Blandin, J. Physique **41**, 193 (1980).

⁷L. I. Glazman and K. A. Matveev, Zh. Éksp. Teor. Fiz. **98**, 1834 (1990) [Sov. Phys. JETP **71**, 1031 (1990)].

⁸K. Flensberg, Phys. Rev. B **48**, 11 156 (1993).

⁹K. A. Matveev, Phys. Rev. B **51**, 1743 (1995).

¹⁰V. J. Emery and S. Kivelson, Phys. Rev. B **46**, 10 812 (1992); D.

G. Clarke, T. Giamarchi, and B. I. Shraiman, *ibid.* **48**, 7070 (1993); A. M. Sengupta and A. Georges, *ibid.* **49**, 10 020 (1994).

¹¹D. Berman, N. B. Zhitenev, R. C. Ashoori, and M. Shayegan, Phys. Rev. Lett. **82**, 161 (1999).

¹²N. C. van der Vaart, A. T. Johnson, L. P. Kouwenhoven, D. J. Mass, W. de Jong, M. P. de Ruyter Van Steveninck, A. van Euden, C. J. P. M. Harmans, and C. T. Foxon, Phys. B **189**, 99 (1993).

¹³I. L. Aleiner, P. W. Brouwer, and L. I. Glazman, cond-mat/0103008 (unpublished).

¹⁴K. Le Hur, Phys. Rev. B **64**, 161302(R) (2001).

¹⁵M. Fabrizio, A. O. Gogolin, and Ph. Nozières, Phys. Rev. B **51**, 16 088 (1995).

¹⁶J. Ye, Nucl. Phys. B **512**, 543 (1998).

¹⁷A. Furusaki and K. A. Matveev, Phys. Rev. B **52**, 16 676 (1995).

¹⁸M. Büttiker, Phys. Rev. B **41**, R7906 (1990).

¹⁹L. I. Glazman, G. B. Lesovik, D. E. Khmel'nitskii, and R. I. Shekhter, Pis'ma Zh. Éksp. Teor. Fiz. **48**, 218 (1988) [JETP Lett. **48**, 238 (1988)].

²⁰F. D. M. Haldane, J. Phys. C **14**, 2585 (1981).

²¹M. P. A. Fisher and L. I. Glazman, in *Mesoscopic Electron Trans-*

- port, Vol. 345 of *NATO Advanced Study Institute, Series E: Applied Sciences*, edited by L. Kouwenhoven, G. Schoen, and L. Sohn (Kluwer, Dordrecht, 1997); also cond-mat/9610037.
- ²²I. L. Aleiner and L. I. Glazman, *Phys. Rev. B* **57**, 9608 (1998).
- ²³M. Büttiker, H. Thomas, and A. Prêtre, *Phys. Lett. A* **180**, 364 (1993).
- ²⁴V. A. Gopar, P. A. Mello, and M. Büttiker, *Phys. Rev. Lett.* **77**, 3005 (1996).
- ²⁵A. O. Gogolin, A. A. Nersisyan, and A. M. Tsvelik, *Bosonization and Strongly Correlated Systems* (Cambridge University Press, Cambridge, UK, 1998).
- ²⁶For $\omega \ll \Gamma_k$, the impurity density of states becomes frequency independent, i.e., $n_k(\omega) = 1/\Gamma_k$. This explains why the frequencies smaller than $\omega_{min} = \max(\Gamma_b, \Gamma_a)$ do not contribute to the (main) logarithmic part of $\delta\epsilon$.
- ²⁷Ph. Nozières, *J. Low Temp. Phys.* **17**, 31 (1974).
- ²⁸Yu. V. Nazarov, *Phys. Rev. Lett.* **82**, 1245 (1999).
- ²⁹C. L. Kane and M. P. A. Fisher, *Phys. Rev. B* **46**, 15 233 (1992).
- ³⁰ $N=1/2$ is generally the condition for resonant tunneling through a double-barrier structure. A. Furusaki and N. Nagaosa, *Phys. Rev. B* **47**, 3827 (1993).
- ³¹E. Lebanon, A. Schiller, and V. Zevin, cond-mat/0110335 (unpublished).
- ³²A. M. Tsvelik and P. B. Wiegmann, *Z. Phys. B: Condens. Matter* **54**, 201 (1984).
- ³³N. Andrei and C. Destri, *Phys. Rev. Lett.* **52**, 364 (1984).
- ³⁴P. Coleman and A. J. Schofield, *Phys. Rev. Lett.* **75**, 2184 (1995); for more details on the method, see P. Coleman, L. B. Ioffe, and A. M. Tsvelik, *Phys. Rev. B* **52**, 6611 (1995).
- ³⁵N. Andrei and A. Jerez, *Phys. Rev. Lett.* **74**, 4507 (1994).
- ³⁶I. Affleck, A. W. W. Ludwig, H. B. Pang, and D. L. Cox, *Phys. Rev. B* **45**, 7918 (1992).
- ³⁷L. I. Glazman, F. W. J. Hekking, and A. I. Larkin, *Phys. Rev. Lett.* **83**, 1830 (1999).